ELSEVIER

Journal of Pharmaceutical and Biomedical Analysis
25 (2001) 239–256

JOURNAL OF
PHARMACEUTICAL
AND BIOMEDICAL
ANALYSIS

www.elsevier.com/locate/jpba

Measurement of potency and lipids in monensin fermentation broth by near-infrared spectroscopy

Robert A. Forbes *, Matthew Z. Luo, David R. Smith

Lilly Research Laboratories, A Division of Eli Lilly and Company, Indianapolis, IN 46285, USA

Received 25 April 2000; received in revised form 2 October 2000; accepted 9 October 2000

Abstract

A transmission near-infrared (NIR) spectroscopic method for quantification of potency and lipids in monensin fermentation broth was developed and validated. Two multiple linear regression calibration curves were established for a set of 100 fermentation samples, correlating the appropriate absorption bands in the NIR spectrum to the laboratory reference methods; high-performance liquid chromatography for potency, and chloroform extraction for lipids. During method development, potency was found to be well correlated to NIR absorbances specific for monensin. While acceptable, correlation of NIR absorbances characteristic of oil to the chloroform lipid method was weaker due to a greater amount of relative variation in the lipid measurements. Following establishment of the optimal calibration curves, the NIR method for potency and lipids was validated for selectivity, accuracy, precision, and robustness. In order to investigate long-term drift in the measurement system, samples were tested both by the NIR and the reference methods over a 7-month period. The differences between results from the two measurements were calculated and statistically analyzed.

Keywords: Transmission near-infrared spectroscopy; Analytical method validation; Monensin fermentation broth; Multiple linear regression; Pharmaceutical analysis; Ionophore; Chemometrics

1. Introduction

Several examples of the use of near-infrared (NIR) spectroscopy in the analysis of fermentation broth have been reported in the literature. Vaccari et al., utilized an online NIR instrument, equipped with a flow cell, to monitor the production of lactic acid in a fermentation of *Lactobacillus casei* [1]. Macaloney et al., demonstrated the ability to quantify four components simultaneously during a recombinant *Escherichia coli* batch-fed fermentation [2]. Simply placing the whole broth in a 0.5 mm quartz cuvette, they measured biomass and concentrations of glycerol (g/l), ammonium (mM), and acetate(g/l) by transmission NIR using four multiple linear regression (MLR) calibration equations established for second-derivative spectra. Also utilizing transmission NIR (but with a 2.0 mm cuvette) and second derivative spectra, Yano et al. developed MLR

* Corresponding author. Tel.: +1-765-8324394; fax: +1-765-8324799.
E-mail address: forbes_robert_a@lilly.com (R.A. Forbes).

0731-7085/01/$ - see front matter
PII: S0731-7085(00)00497-0

calibrations for ethanol and acetic acid for a rice vinegar fermentation [3]. They utilized a clever approach to ensure the method was selective by preparing synthetic mixtures of ethanol and acetic acid standards, holding one component constant and varying the concentration of the other. Examining overlays of second-derivative spectra for these samples, they chose as calibration wavelengths those peaks that increased with increasing analyte concentration, but were also cross-over (zero) points for spectra with varying concentrations of the other analyte. As a result, their MLR calibration equations were robust to variation in the concentrations of the other component. Brimmer and Hall developed a method to quantitate a nutrient oil in fermentation broth using reflectance, second-derivative, NIR with MLR [4]. They found that the predictive ability of the model improved significantly when they divided the response of the oil band at 1720 nm by a second wavelength that they believed to provide scatter correction.

The advantages of utilization of near-infrared technology in the analysis of fermentation broth samples are manifold. More than one analyte concentration may be calculated from the same NIR spectrum, allowing replacement of several separate test methods by one analysis. Direct

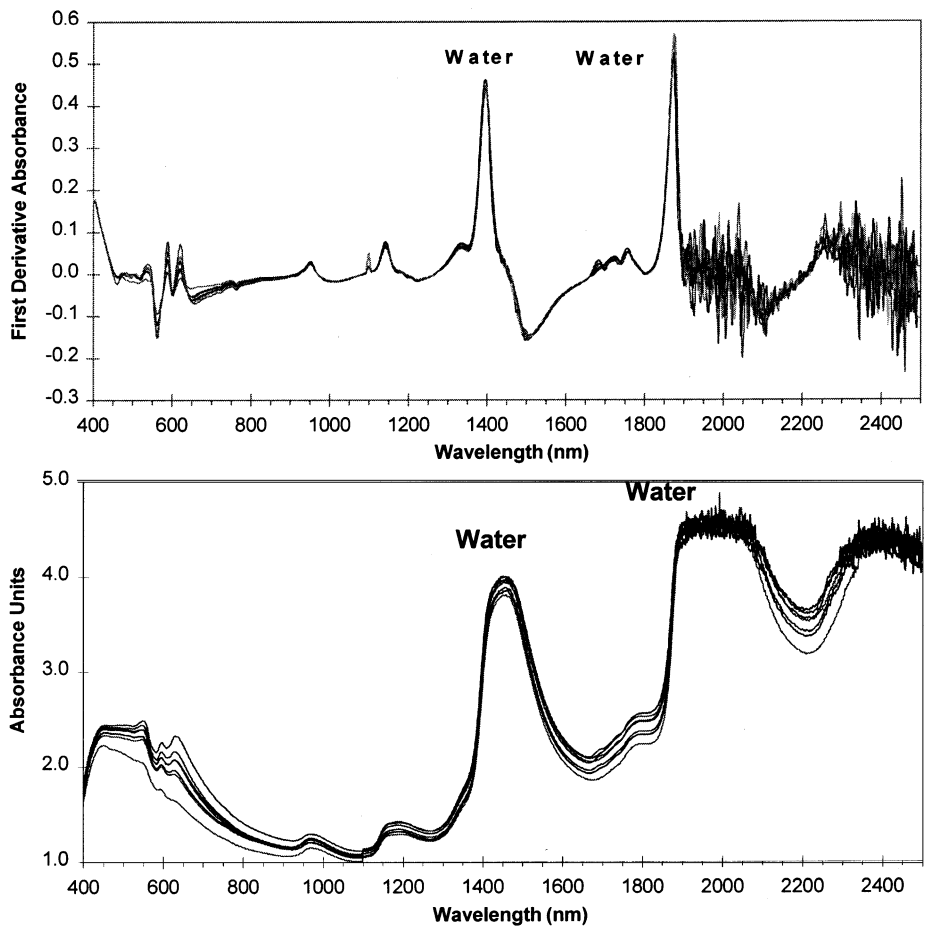

Fig. 1. Transmission NIR spectra for monensin fermentation broth samples with various ages/potencies. The top overlay shows the first-derivative spectra and the bottom overlay shows the primary spectra. Note that the jagged lines centered around 2000 and 2400 nm indicate spectral noise due to the sample absorbing essentially all the radiation here.

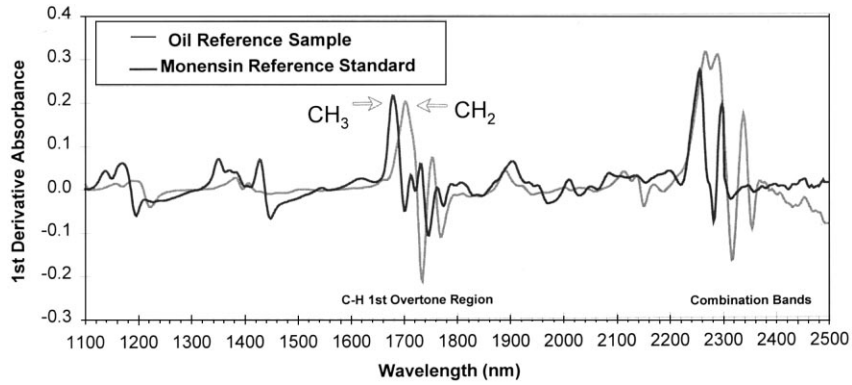

Fig. 2. NIR spectra obtained for the monensin reference standard and a reference sample of the oil mixture used in its fermentation. The spectrum for the crystalline monensin reference standard was obtained in reflectance mode and the spectra have been adjusted to approximately the same scale for comparison purposes.

Table 1
Influence of oil and monensin spikes on NIR results for potency and lipid

Number	Sample identification	Oil spike (mg/g)	Monensin spike (mg/g)	ΔNIR potency (mg/g)	ΔNIR lipid (mg/g)
1	Batch A+oil	+6.8	0	−0.3	11.6
2	Batch B+oil	+6.5	0	1.7	8.4
3	Batch C+oil	+7.8	0	−0.5	8.2
4	Batch A+monensin	0	+8.3	8.5	2.9
5	Batch B+monensin	0	+6.5	9.9	3.3
6	Batch C+monensin	0	+8.8	9.2	4.1

Table 2
Effect of added monensin on NIR results for lipid in fermentation broth

Number	Sample identification	Monensin spike (mg/g)	ΔNIR potency (mg/g)	ΔNIR lipid (mg/g)
1	Batch D+monensin	+4.2	3.9	−1.7
2	Batch E+monensin	+4.2	6.6	3.2
3	Batch F+monensin	+4.2	4.9	3.3
4	Batch G (control)	0	0.0	−0.4
5	Batch H (control)	0	0.1	0.8
6	Batch I (control)	0	1.2	0.4
7	Batch G+monensin	+4.2	3.1	1.0
8	Batch H+monensin	+4.2	1.2	−0.7
9	Batch I+monensin	+4.2	4.8	3.0

measurement of the entire sample eliminates the loss of the analyte during extraction and/or clean-up (e.g. filtration) steps. Elimination of method steps, such as weighing, volumetric dilution, chromatography, peak integration and calculation versus a similarly prepared standard, has the potential to improve overall method precision. NIR results are generated in a matter of minutes, as opposed to hours for the laboratory reference methods.

Along with these advantages, the limitations of NIR analysis are important to consider. The vi-

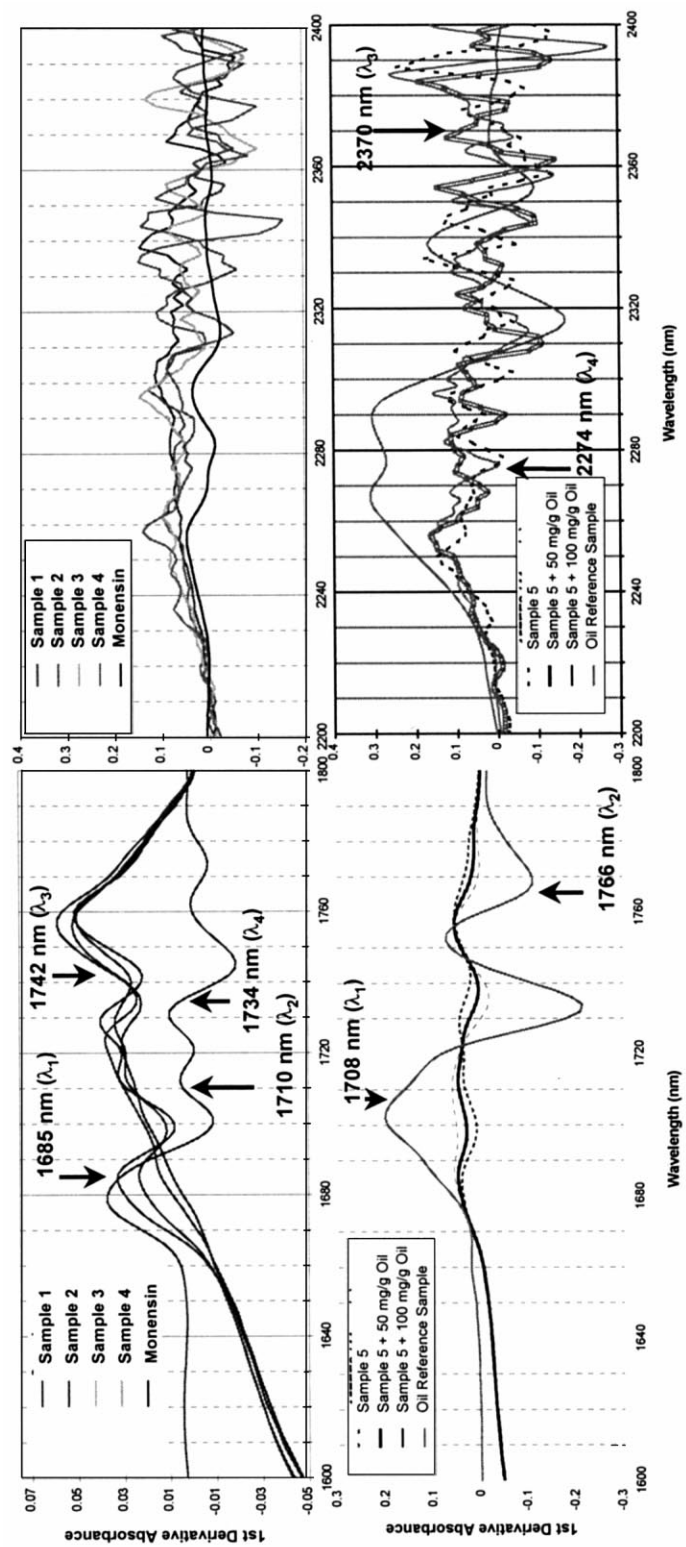

Fig. 3. Overlay of first-derivative NIR spectra obtained for monensin fermentation broth samples with various ages/potencies with spectra obtained for the monensin reference standard (reflectance mode) and an oil reference sample. The wavelengths utilized to build the MLR models have been indicated. Note that the height of the 1685 nm band increases with increasing monensin potency. Also note that the spectra have been adjusted to approximately the same scale for comparison purposes.

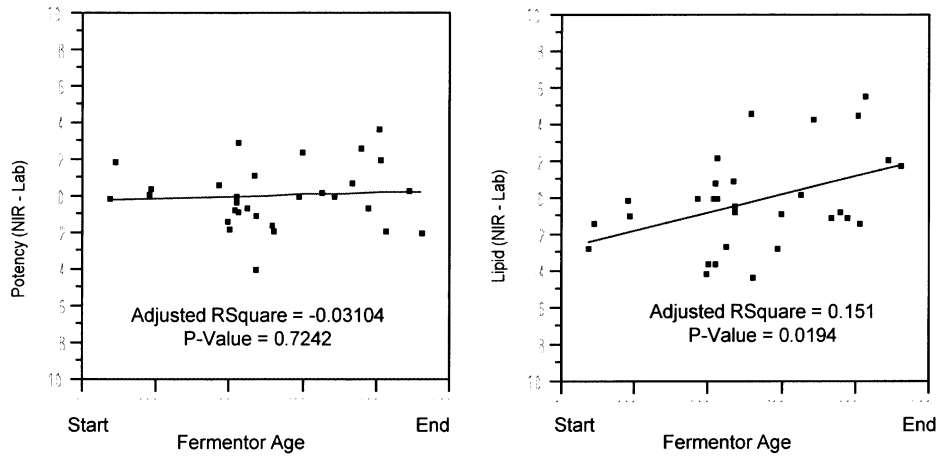

Fig. 4. Residuals for potency and lipid assays (NIR − laboratory reference) (in mg/g) regressed against fermentor age for a set of monensin broth samples.

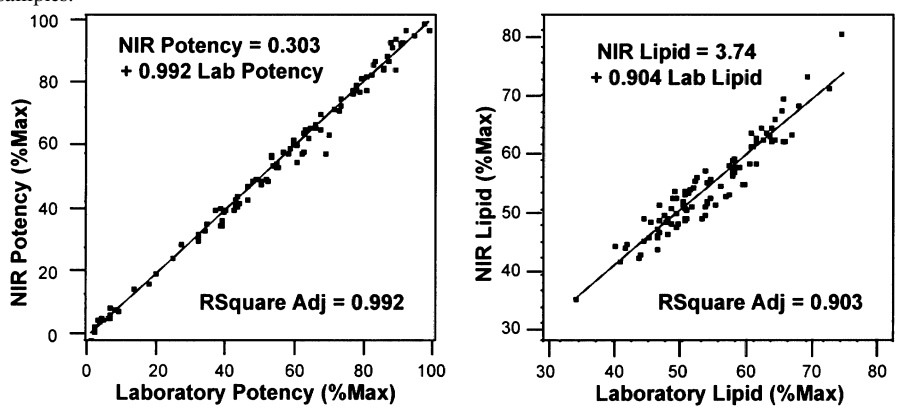

Fig. 5. Linear regression analysis for NIR potency and NIR lipids versus laboratory reference assays. Note: the scales have been adjusted to percent of the maximum potency value.

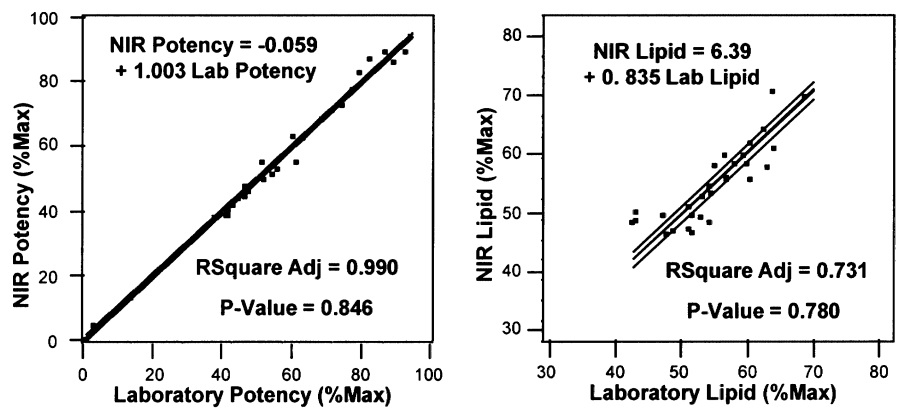

Fig. 6. Linear regression analysis and paired *t*-test for potency and lipid content of monensin broth by NIR versus laboratory reference results for the accuracy validation set. Note: the scales have been adjusted to percent of the maximum potency value.

Table 3
Summary statistical analysis of data obtained in full-factorial screening design of experiments (DOE)[a]

Term	Whole model potency		Whole model lipid	
	Estimate	Prob $>\|t\|$	Estimate	Prob $>\|t\|$
Sample batch	*4.16*	*<0.0001*	*9.347*	*<0.0001*
Homogenization	0.12	0.360	*0.749*	*0.001*
Sample batch × homogenization	−0.12	0.373	*0.471*	*0.027*
Sample agitation	*0.67*	*0.000*	*0.465*	*0.028*
Sample batch × sample agitation	−0.21	0.124	−0.249	0.216
Homogenization × sample agitation	−0.07	0.592	−0.298	0.142
Cuvette	−0.16	0.242	0.312	0.125
Sample batch × cuvette	*0.26*	*0.064*	*0.387*	*0.062*
Homogenization × cuvette	0.23	0.101	0.145	0.462
Sample agitation × cuvette	−0.14	0.317	−0.323	0.113
Temperature	−0.07	0.579	0.225	0.261
Sample batch × temperature	*0.30*	*0.038*	*0.493*	*0.021*
Homogenization × temperature	0.01	0.923	0.091	0.642
Sample agitation × temperature	−0.03	0.814	0.057	0.771
Cuvette × temperature	*−0.29*	*0.044*	−0.316	0.121

[a] Parameters in italics are those found significant at a 90% confidence ($P<0.10$). Prob, Probability.

Table 4
Statistical analysis of data obtained for sample A and sample B analyzed separately[a]

Term	Sample A Potency		Sample B Potency		Sample A Lipid		Sample B Lipid	
	Estimate	Prob $>\|t\|$	Estimate	Prob $>\|t\|$	Estimate	Prob $>\|t\|$	Estimate	Prob $>\|t\|$
Tissumize	0.25	0.273	0.00	0.970	0.28	0.126	*1.22*	*0.016*
Agitation	*0.88*	*0.007*	*0.45*	*0.004*	*0.71*	*0.005*	0.22	0.557
Tissumize × agitation	−0.32	0.166	*0.18*	*0.098*	*−0.31*	*0.093*	−0.28	0.451
Cuvette	*−0.42*	*0.087*	0.10	0.298	−0.08	0.641	*0.70*	*0.098*
Tissumize × cuvette	*0.42*	*0.088*	0.04	0.688	−0.20	0.236	0.50	0.209
Agitation × cuvette	0.08	0.702	*−0.35*	*0.010*	−0.19	0.258	−0.45	0.245
Temperature	−0.37	0.120	*0.22*	*0.052*	−0.27	0.138	*0.72*	*0.091*
Tissumize × temperature	−0.10	0.636	0.13	0.210	−0.05	0.737	0.24	0.522
Agitation × temperature	−0.01	0.957	−0.05	0.581	0.06	0.709	0.05	0.881
Cuvette × temperature	−0.27	0.228	*−0.30*	*0.018*	−0.03	0.850	−0.60	0.141

[a] Italics highlight those parameters found significant at a 90% confidence ($P<0.10$). Prob, Probability.

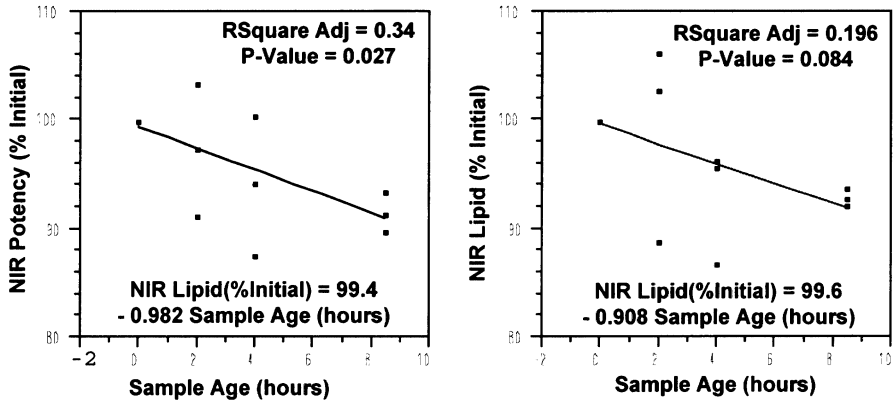

Fig. 7. Linear regression analysis of percent initial potency and lipid content versus time at room temperature following homogenization for monensin broth samples.

Table 5
Analysis of variance components for the monensin broth NIR method

Component	Potency			Lipid		
	Variance estimate	% of total	Probability $>F$	Variance estimate	% of total	Probability $>F$
Sample batch	54.105	97.4	<0.0001	1.033	35.7	<0.0001
Analyst (sample number)	-0.634	0.0	0.9922	-0.243	0.0	0.6286
Error	1.437	2.6		1.863	64.3	

brations that give rise to overtone and combination absorbances falling in the NIR region are predominantly those involving the bonds of hydrogen to a heteroatom such as carbon, nitrogen, oxygen, etc. Thus, compounds that do not contain hydrogen, such as inorganics, do not give rise to an appreciable NIR spectrum. NIR absorbances arise from combinations and harmonics of the fundamental IR absorbances, and are generally one to several orders of magnitude weaker. This effect, which allows direct sample analysis, sacrifices sensitivity to analytes at trace concentrations.

Near-infrared spectra are affected not only by changes in chemical concentration, but also by changes in physical properties. During a typical fermentation, total solids change due to organism growth, changing the viscosity and turbidity of the sample. These effects change the light-scattering properties. Such sample matrix effects have consequences on the NIR spectra, including baseline offsets among spectra. In addition to mathematical manipulation of the spectra (e.g. derivative spectroscopy), Hammond and Brookes published an approach to compensate for these changes using multiple calibration curves (segments) depending on tank age [5]. To investigate, understand, and address these limitations, rigorous analytical method validation is crucial to test the veracity and robustness of the measurement [6]. The selectivity, linearity, accuracy, sensitivity, and precision of a method must be thoroughly tested and documented. Care must be taken to ensure the calibration is founded upon spectral information specific for the analyte, since it is possible to establish calibrations that appear to be valid based upon unrelated but correlated information [7]. Specificity for the analyte of in-

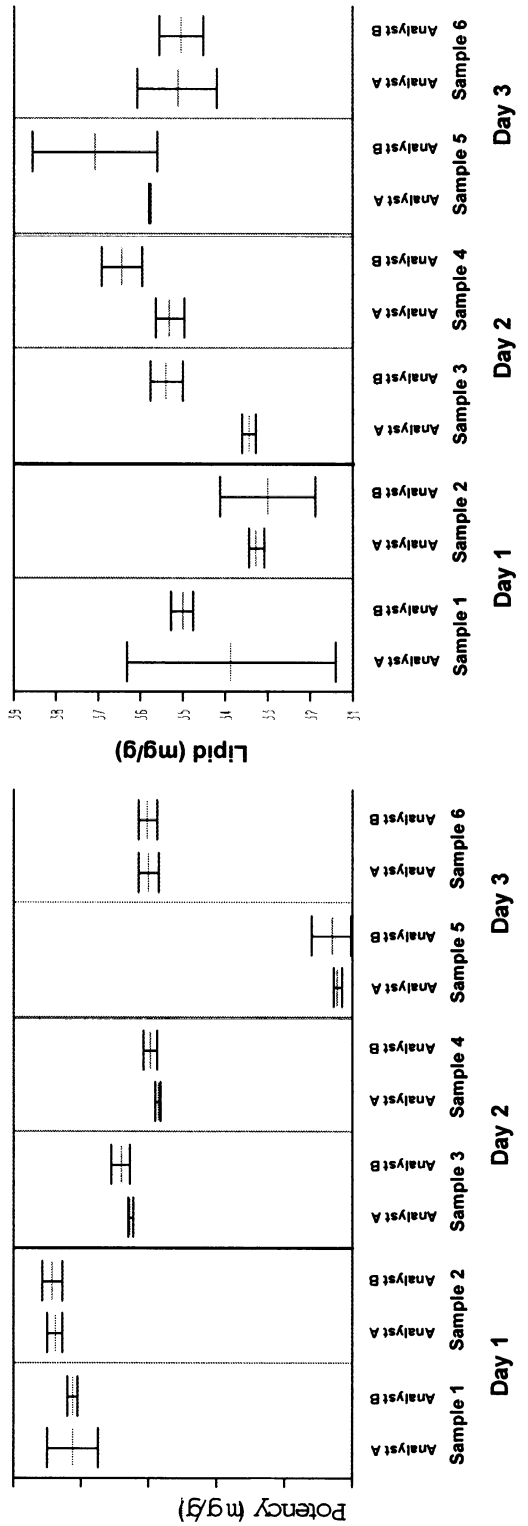

Fig. 8. Variability chart showing relative contribution of analyst, day, and replication to the intermediate precision of the method for potency and lipid content in monensin broth by NIR.

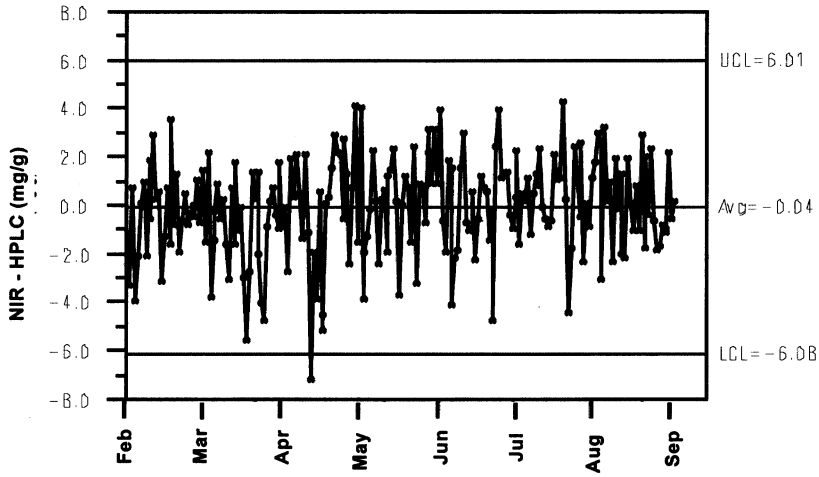

Fig. 9. X-Chart analysis of the residuals obtained for the monensin broth samples analyzed by HPLC and NIR for potency over a 7-month period.

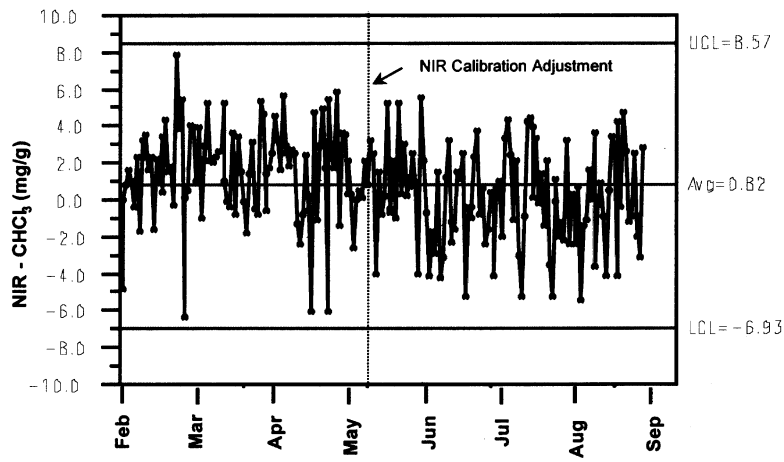

Fig. 10. X-Chart analysis of the residuals obtained for the monensin broth samples analyzed by the gravimetric method and by NIR for lipid content over a 7-month period.

terest must be assured by recording the spectra for known standards along with the sample (blank) matrix components. Development of the calibration curve by correlation to a primary method will simultaneously validate the linearity of the method. Accuracy must be assessed by a separate set of samples, unrelated to those used for calibration development. Precision and robustness are assessed by designed experiments that examine the influence of instrumental parameters, analyst technique, and batch-to-batch variation on the measurement and to determine the intermediate precision of the method.

Following validation, the method should be monitored on an ongoing basis to check for drift in the entire measurement system. This drift might include loss in instrument/detector sensitivity with age, and/or changes in the sample matrix, such as a change in the source/vendor of a fermentation raw material. Instantaneous changes, such as in-

strument source lamp replacement, repairs, or changes to the fermentation process that affect the sample, must also be addressed. One strategy to assure the ongoing accuracy of the NIR calibration is to perform the reference method on some fraction of samples over time. The difference between the NIR and reference measurements can be calculated and analyzed by statistical control charting to test for drift in the measurement system and/or special cause variation.

Monensin (**1**) is a naturally occurring macrocyclic ionophore produced by fermentation of the microorganism *Streptomyces cinnamonensis* [8]. Monensin is the active ingredient in the animal feed additives Coban® and Rumensin®, marketed by Elanco™ Animal Health as growth promoters. In order to investigate potential advantages and limitations, a NIR method was developed to quantify potency and lipids in monensin fermentation broth samples.

2. Experimental

2.1. Theory

In transmittance mode, the NIR beam passes from the source and optics through the sample, and is measured by a transmission detector. For a single-beam instrument, a background or reference spectrum is first obtained by measurement of the empty sample cell. The sample spectrum is then compared with the reference spectrum and converted to absorbance, A, defined by:

$$A = \log[1/T] \tag{1}$$

where transmittance $T = I_S/I_R$, and I_R is reference intensity and I_S sample intensity. For solutions, sample absorbance, at a wavelength where a given analyte has a chromophore that absorbs some radiation, is related to analyte concentration by the familiar Beer's Law relationship [9]:

$$A = \varepsilon(\lambda)\cdot b\cdot c \tag{2}$$

where $\varepsilon(\lambda)$ is the molar absorptivity (extinction coefficient) of the analyte at the specific wavelength λ, b is the path length, and c is the concentration of the analyte. This relationship may be considered a first approximation in systems, such as fermentation broth samples, where light is also lost due to scattering by suspended particles. Using the convention of Martens and Naes, the relationship between absorbance and concentration, shown in Eq. (2), is said to be reverse causality, i.e. A is caused by c [10]. The objective of the calibration model is to predict c from a measured A. This is achieved by least-squares regression of concentration versus absorbance in a forward (also called inverse) regression of c versus A. Since a given analyte typically absorbs at more than one wavelength, the spectra contain collinear information. As one approach to deal with collinearity, and to establish the calibration curves to allow prediction of the concentrations of the two analytes from the NIR spectra, a stepwise MLR approach was utilized [11]. A variant of this approach, suggested by the instrument vendor, was to utilize a ratio of two wavelengths as each term for the MLR equation [12]. With this approach, the wavelength (λ_1) with the highest correlation to the analyte, while considering the spectral noise (sensitivity parameter), would be selected as the numerator. During the next iteration, an optimal denominator (λ_2) for the first wavelength was sought, generally limiting the selection range to $\lambda_1 \pm 100$ nm. The general rationale for division was to provide scatter correction by dividing by a nonabsorbing wavelength. Selection of further wavelengths and/or ratios was continued until the improvements to the model were considered to be minimal. The general form of the calibration equation using this approach was:

$$c = a_0 + a_1\frac{\lambda_1}{\lambda_2} + a_2\frac{\lambda_3}{\lambda_4} + a_3\frac{\lambda_5}{\lambda_6} + \ldots \tag{3}$$

where a_0 is the intercept, and a_1, a_2, and a_3 are the constants resulting from the linear regression correlation to the laboratory reference method results. λ_1 symbolizes the absorbance at the first wavelength.

In order to improve the selectivity of the method, instead of allowing an empirical selection of the wavelength with the highest correlation to each analyte, the relative maximum of a peak

observed in the samples, which was known to be specific for the analyte, was selected as λ_1. These peaks were identified by examining spectra obtained for authentic reference samples, and were generally found to be highly (albeit not usually maximally) correlated to the reference method values for the analyte.

Standard regression models were developed using primary spectra, first-derivative spectra and second-derivative spectra. First-derivative spectra were found to correlate better to the analytes of interest. Derivatization visibly enhanced the resolution of neighboring peaks and eliminated baseline offset between samples. Thus, all spectra were converted to the first derivative for this work.

During development, the performance of a given calibration model with respect to fitting the calibration spectra was assessed by the statistical measures provided by the instrument software NSAS™ version 3.52 [13], the correlation coefficient (R) and the standard error of calibration (SEC) given by:

$$R = \left[\sum (Y_{\mathrm{NIRS}} - \overline{Y})^2 / \sum (Y_{\mathrm{REF}} - \overline{Y})^2 \right]^{1/2} \quad (4)$$

and

$$\mathrm{SEC} = \left[\sum (Y_{\mathrm{NIRS}} - Y_{\mathrm{REF}})^2 / (n - m - 1) \right]^{1/2} \quad (5)$$

Similarly, the performance of the calibration models with respect to fitting the validation set spectra was assessed the standard error of prediction (SEP) given by:

$$\mathrm{SEP} = \left[\sum (Y_{\mathrm{NIRS}} - Y_{\mathrm{REF}})2 \right] / (n-1)^{1/2} \quad (6)$$

where Y_{NIRS} is the NIRS predicted result for the sample, Y_{REF} the reference method result for the sample, $\overline{Y}$ the average of reference method results for samples, n the number of samples and m is the number of independent variables.

In addition to the calculations provided with the NSAS software, the software package, JMP™ version 3.2.2 (SAS Institute, Inc.) for Windows 95™ was utilized to perform other standard statistical analyses of the analytical method validation results.

2.2. Instrumental

A Foss NIRSystems, Inc. model 6500 instrument equipped with a Multimode™ (registered trademark of Foss NIRSystems, Silver Spring, MD) liquid/solid sample accessory has been utilized for all NIR measurements. The spectral acquisition range was 400–2500 nm, which included the visible region (400–1100 nm) and NIR region (1100–2500 nm). A quartz cuvette with a 2 mm path length was utilized for all transmission measurements. The samples were too viscous to fill a 1 mm cuvette, and path lengths greater than 2 mm attenuated the signal too greatly in the NIR range.

For each spectrum, 32 scans were averaged and the spectra were pre-processed prior to calibration by conversion to first derivative, utilizing a three-point digital smoothing (moving average with a gap of zero and a segment size of 6 nm) with NSAS. Unsmoothed spectra, three-point-smoothed, and five-point-smoothed second-derivative spectra were visually compared in order to examine the effect of the smoothing parameter. Three points, which was the minimum smoothing possible, was chosen as optimal, providing some noise reduction without distorting the spectra (i.e. loss of resolution between neighboring peaks, shifting of peak maxima, etc.).

2.3. Materials and method

Spectra for 100 fermentation samples were acquired over a period of several months for the calibration set/library. These 100 samples were obtained from 57 separate fermentation runs and represented various fermentor ages. Simultaneously, spectra for 30 additional samples, from 26 separate fermentations, were acquired for use as the validation/test set. Twelve of the test set samples were obtained from fermentation runs also represented in the calibration set, albeit from samples taken at different fermentor ages. A sample of the oil utilized for the fermentation was obtained and used as an oil reference sample. A sample of crystalline monensin, sodium salt, (Eli Lilly and Company, Indianapolis, IN) was utilized as a reference standard for monensin.

Prior to performing the laboratory reference methods, all samples were homogenized for 1 min using a laboratory homogenizer (Tissumizer®; Tekmar Company, Cincinnati, OH). The laboratory reference method for potency was high-performance liquid chromatography with post-column derivatization with vanillin reagent (HPLC/PCD) [14]. The laboratory reference method for lipid content was a gravimetric method. Fermentation broth was extracted with an acidified organic solvent, the extractant was filtered, and the filtrate was evaporated/dried to constant weight in a vacuum oven. Since monensin was also extracted along with the lipids, the monensin potency was subtracted from the total amount of extracted material.

NIR spectra were recorded following analysis by the laboratory reference methods. Just prior to analysis, samples were agitated by shaking the sample bottle, the 2 mm cuvette was filled with sample by means of a disposable, Teflon transfer pipette, and the cuvette was placed into the cell holder in the instrument, which was maintained at 37°C. The sample was allowed to equilibrate to constant temperature for 60 s prior to recording the NIR spectrum.

3. Results and discussion

3.1. Selection of the optimum calibration model

A visual comparison of the effects of derivatization as a mathematical preprocessing treatment is shown in Fig. 1 for spectra from monensin broth samples selected to represent a wide range in potency. It should be noted that the wavelengths higher than about 1900 nm exhibited greater spectral noise caused by nearly complete absorbance at the higher wavelengths. The large absorbance at around 2000 nm was assigned to the combination band for water, the primary component of the samples.

The first-derivative NIR spectra obtained for reference samples of the two analytes of interest are shown in Fig. 2. Comparing the spectra obtained for the samples in Fig. 1 with the spectra obtained for the analytes in Fig. 2, it was apparent that the C–H overtone region (1600–1800 nm) contained useful spectral absorbances due to the analytes, which were not obscured by the strong absorbances due to water. Derivatization of the spectra enhanced the resolution of the neighboring peaks in this region. Although the absorbances due to monensin still overlapped with those due to the oil, derivatization improved their separation, and this would be expected to improve the selectivity of the method (see Fig. 3).

Using the approach described in Section 2, λ_1 was forced to 1685 nm, which was the relative maximum of a peak observed in the samples in the C–H overtone region corresponding to the CH_3 region (see Fig. 3, top). This peak was observed to increase as the potency of the sample increased. Presumably, this peak arose from the absorbance of the methyl groups present in monensin. The denominator wavelength providing the optimum improvement to the calibration (1710 nm) was selected from the range 1600–1800nm. Remarkably, this was nearly the same as the wavelength used in the first term for lipid content. This suggested that the denominator was, in fact, providing a correction for lipid content of the samples. This would be expected to improve the calibration if lipids contributed to the absorbance at 1685nm. The spectra shown in Fig. 3 supported this. The software was allowed to automatically select 1742 nm as a third wavelength, which empirically provided the best improvement to the model fit. Again allowing automatic selection (with the range constrained to 1600–1800 nm), 1734 nm was found to be its optimal denominator.

While building MLR models such as this one, addition of terms generally always improved R and SEC for the calibration spectra. To test for over-fitting the spectra (improvement of the fit due to chance correlations), the validation/test spectra were utilized. When the second term (1742 nm/1734 nm) was added to the potency calibration model, R and SEC improved for the calibration spectra, and SEP and R improved for the validation samples. However, when a third term was added, which improved the fit to the calibration spectra, SEP and R for the validation samples did not improve. This indicated the

three-term model was overfitting the data. Thus, the optimal calibration for monensin potency was found to be:

$$C_m = -10.62 + 71.34\frac{A_{1685}}{A_{1710}} - 10.01\frac{A_{1742}}{A_{1734}} \quad (7)$$

In a similar manner, the optimal calibration for lipid content was found to be:

$$C_l = -15.53 + 86.97\frac{A_{1708}}{A_{1766}} + 0.77\frac{A_{2370}}{A_{2274}} \quad (8)$$

where C_m is the concentration of monensin (mg/g), C_l is the concentration of lipid (mg/g), and A_{1685} is the first-derivative absorbance at 1685 nm. Again, further terms did not improve the model. The relative maximum of a peak observed in the samples in the C–H overtone region corresponding to the CH_2 region was 1708 nm (see Fig. 3, bottom). Presumably, this peak arose due to the absorbance of the methylene groups present in the oils and triglycerides that comprise the lipids. It should be noted that the second term in the model for lipids utilized wavelengths from a region with relatively high spectral noise. While the coefficient for this term was about two orders of magnitude less than the coefficient for the first term (making it much less influential on the model), given the noise in this region, it was remarkable that this term improved (albeit perhaps marginally) the fit of the NIR spectra the chloroform lipid data. Spectral noise was a concern due to the possibility that the denominator could approach zero, causing this second term to have a large effect on the result.

3.2. Validation of selectivity

The selectivity of the method was established during calibration by judicious selection of wavelengths that were specific for the analyte in the presence of the other sample matrix components. However, it was important to realize that, during the course of fermentation, the sample matrix changed with fermentor age: the biomass increased, monensin potency increased, and lipid content also changed. To test for the effect of these changes in the sample matrix on the NIR measurement, the residuals (NIR method minus laboratory reference method) were plotted as a function of tank age (see Fig. 4). No correlation of the residual for potency with age was observed, demonstrating good selectivity of the NIR method for monensin in the changing sample matrix. A small, but significant, correlation of the residual for lipids to tank age was observed. Residuals were higher for samples of higher age (higher monensin potency).

To further investigate the selectivity of the method, samples from three different fermentors were spiked with the oil reference sample and separately with the monensin reference standard, followed by NIR analysis. This was not intended as a spike/recovery study, but simply to investigate the effect of changes in the matrix components on the analyte concentration predicted by the NIR calibration. Percent recoveries were not calculated, since the standards used for spiking were in a different form than normally found in authentic fermentation samples. NIR is well known to be sensitive to such differences (i.e. crystalline versus amorphous/solubilized monensin, feed versus metabolized oil). The results of the spiking study are presented in Table 1.

When oil was added to the samples, a consistent increase in the lipid result was obtained, indicating the NIR method was indeed quantifying oil as lipid. Similarly, a consistent increase in potency was obtained when the reference standard was added to the samples.

For all three samples, spiking with oil did not significantly change the potency result; the differences (spiked versus original) were all less than two standard deviations (± 2.4 mg/g). This demonstrated excellent selectivity of the method for monensin in the presence of varying amounts of the lipids. However, when the samples were spiked with monensin, lipid results increased for all three of the samples. To better understand the impact of spiked monensin on the lipid results, this experiment was repeated for six more fermentation samples. Three preparations were made as controls, which were handled in the same manner as the spikes, albeit without added monensin, testing the impact of the spiking procedure itself. The results of the repeated experiment, shown in Table 2, were consistent with the first.

On average, the lipid result increased when samples were spiked with 10–20% additional monensin; the average increase of about 2 mg/g was statistically significantly different from zero. This increase was consistent with the positive slope of the line shown in Fig. 4. The results obtained for the controls did not suggest that sample handling during spiking caused the increase.

The cause for the increase in lipid result with increased monensin potency may be explained by a closer examination of Fig. 3. The monensin standard exhibited a positive, first-derivative absorbance at 1708 nm, perhaps due to the methylene groups present in monensin. Thus, the NIR band at 1708 nm was the sum of the absorbance due to the oils with a contribution from monensin. By calibrating the NIR method to the laboratory method for lipids, the average effect was reduced to zero. Since the correlation shown in Fig. 4 was weak, due to other sources of variation in the system, the selectivity of the method for lipids in the presence of monensin, while not ideal, was considered to be adequate.

3.3. Validation of linearity

In order to assess the linearity of the NIR method over the range of analyte concentrations present in the calibration set, the NIR results were plotted versus the laboratory reference method results, and a correlation coefficient was calculated. A correlation coefficient (adjusted R-squared) of 0.992 was obtained for monensin potency, and a correlation coefficient of 0.903 was obtained for lipid content. This demonstrated linearity over the potency range of interest, and the lipid content range of interest. While a larger correlation coefficient for lipids was desirable, an important consideration here was that the noise introduced by both the NIR measurement and the reference measurement (gravimetric method) both contributed to scatter in the calibration line. Not only does the noise in the reference measurement reduce the correlation coefficient, but it can actually cause the slope to be underestimated [15]. When the laboratory results for potency and/or lipids are regressed to the NIR results, the slopes are both unity because this was how the calibrations were established (forward/inverse regression). When the regression was inverted (NIR regressed against laboratory results), as shown in Fig. 5, the slope of the best-fit line for potency decreased from 1.000 to 0.992, and the slope for the lipids decreased from 1.000 to 0.904. The former decrease was insignificant; however, the latter decrease in slope was consistent with underestimation due to noise in the dependent variable (laboratory lipid results).

The change in slope of the best-fit line when the regression was inverted illustrates an important limitation of least-squares fitting due to the assumption that no noise will be present in the independent variable. While the current analysis examines the relationship between the NIR method results and the reference method results, the same limitation holds true for the calibration curve, which regresses the reference method results against the absorbances utilized in the MLR equation. This demonstrates the need for instrument manufacturers/developers to incorporate regression methods that are more robust to noise in the variables into their software. One such approach is the unbiased or symmetrical approach described by Mandel [16]. A referee has suggested partial least-squares may be another approach to deal with noise in the independent variables.

3.4. Validation of accuracy

Accuracy was evaluated by testing 30 monensin broth samples that were not utilized in establishing the calibrations. The differences between the NIR results and reference method results (residuals) for each sample were treated in a paired analysis. Results of X-chart analyses and Shapiro–Wilk W tests for normality indicated no special-cause variation was present and the residuals were normally distributed. Following these tests, a paired t-test was performed to test for any bias between the NIR method and the reference methods (see Fig. 6). The paired t-tests showed no statistically significant difference between the methods at a 95% confidence ($P \leq 0.05$). The adjusted R-squared correlation coefficient for potency was 0.990, demonstrating excellent

agreement of the two methods. However, the adjusted R-squared for the lipid data was only 0.731, consistent with the greater relative error in the lipid results. It is important to note that the correlation coefficient was affected by the range in the data. With equivalent noise, a narrow range produces a lower R-square than a wide range. For example, when the best-fit line for lipids in Fig. 6 was forced through the origin (a zero, zero point was included for illustration purposes only), the adjusted R-squared improved to 0.910.

For 30 paired potency differences, the power of the paired t-test to find an actual bias equal to or greater than 1 mg/g was estimated to be 85% for $\alpha = 0.05$ with a standard deviation (of the residuals) of 1.7 mg/g [17]. This means that the chance of not detecting a true 1 mg/g difference as statistically significantly different in this study was 15%. Using the same approach for lipids, the power of the paired t-test to find a bias equal to or greater than 1 mg/g was estimated to be 50% for $\alpha = 0.05$ with a standard deviation of 2.6 mg/g. The power increased to 85% if the lipid difference to be detected was 1.5 mg/g.

3.5. Validation of precision and robustness

To assess the robustness of the NIR method, and to determine which parameters were most important to control, a full factorial screening experimental design was utilized to examine the effect of sample temperature (26–37°C), the cuvette used (cuvette 1 versus cuvette 2), homogenization (no tissumization versus tissumization), and sample agitation (vigorous shake versus gentle swirl) on the NIR results for samples from two different fermentors (sample batches). The results of this study are presented in Table 3.

The interactions of many of the parameters with sample batch suggested that the samples from the two fermentors were affected differently by these parameters. The data was split into two blocks, one for each sample batch, and the blocks analyzed separately. The results of statistical analyses for these data are presented in Table 4.

It was observed that sample B contained foam whereas sample A did not. This might explain the differences in the effect of agitation and homogenization. Homogenization was retained in the method, since the library was established from homogenized samples and at least some samples appeared to be affected by homogenization. The lipid results for sample B, affected by homogenization, decreased an average of 2.4 mg/g with homogenization. Agitation of the sample was important: more vigorous agitation increased both potency ($+1.3$ mg/g) and lipid ($+1$ mg/g), suggesting solids might be settling to the bottom. Since air bubbles were sometimes observed in the samples following vigorous shaking, agitation was standardized to a vigorous swirling, to provide thorough mixing of the sample, without entrainment of air bubbles. The significance of the interactions involving cuvette were not well understood. A physical inspection of the two cuvettes proved them very similar in appearance. The data suggested changing the cuvette might have an effect, possibly due to tolerances around path length during cuvette manufacture. The method should be monitored closely for the need to recalibrate following a change of the cuvette. Temperature was found significant only for sample B, and here the effects were relatively small. This was remarkable considering that an 11°C range was examined for a liquid sample.

Another aspect of the robustness of the method, sample stability, was evaluated by testing samples from three different fermentors initially, and at 2, 4, and 8 h time intervals. The samples were homogenized once, and remained closed in the laboratory at ambient temperature. Calculated as a percent of the initial value, the results obtained for this study have been shown in Fig. 7. While the correlations were relatively weak, these results suggested that the NIR potency and lipid values decreased at a rate of about 1 mg/g/h following homogenization. This study was subsequently repeated, and the same trend noted. This effect, along with the significance of agitation observed in the screening study, was consistent with the hypothesis that solid material in the sample settled out with time, reducing the amount of potency and lipids in the sample cell path.

Based upon the sample stability results, the method was revised to require analysis of the sample within 2 h following homogenization.

With this change, the intermediate precision of the method was determined utilizing a crossed/nested experimental design, which also allowed an analysis of the components of variation. Two different samples each day were tested in duplicate, on each of 3 days, by two analysts. Because samples from different batches were tested each day, due to concerns that a sample might change upon storage for multiple days, the day-to-day contribution to the method variance could not be separated from the batch-to-batch effect. The effects of batch and analyst were determined in a statistical analysis of variance. A visual comparison of the relative effects of these components are shown in Fig. 8. The results of the analysis, presented in Table 5, showed that analyst technique was not statistically significantly different. Sample batch contributed a much greater portion of the variation for potency than lipid, since the batches actually had a wider range in potency than lipid content range.

As an estimate of the intermediate precision of the method, a standard deviation was calculated by taking the square root of the variance for the error term. The sample-batch contribution was excluded because it included batch-to-batch variation, which was not part of the measurement variation. Using this method, the precision of the method was estimated to be 1.20 mg/g as one standard deviation for potency and 1.36 mg/g for lipid. In comparison, the standard deviations of the reference methods for potency and lipid methods (estimated by analysis of the same sample over multiple days) were 1.66 and 1.89 mg/g, respectively.

It should be noted that the standard deviation estimates for the reference methods included a contribution from day-to-day effects, but the precision estimates for the NIR did not effectively include day-to-day variation. Day-to-day variation for the NIR method was not expected to be large, since the same calibration curve (stored in computer memory) was used each day. On the other hand, the effect of preparing and chromatographing standards for the calibration curve would be expected to contribute significant day-to-day variation to the HPLC/PCD method. Also, preparation of batches of lipid extractant (typically utilized for one or more days) would contribute day-to-day variation to the gravimetric method. Thus, the precision of the NIR method was considered to compare favorably with the laboratory reference methods.

3.6. Monitoring the NIR method for long-term drift

In the measurement of monensin fermentation broth, the NIR method was developed as a secondary method, established by correlation to two primary methods. Because of the possibility that the instrumentation and/or the fermentation process might change over time, we chose to study the potential drift in the measurement system. The approach we utilized was to perform both the reference methods, and the NIR method, on a given sample, on a daily basis for a period of 7 months. A scheme was employed to ensure that these samples represented many fermentation batches at various ages. The differences between the NIR and reference method results (residuals) were statistically analyzed by control charting. These control charts were analyzed for statistically significant patterns (e.g. a single value beyond the control limits or non-random patterns/run rules violations such as six points in a row steadily increasing or decreasing) that might indicate drift in the measurement system.

Fig. 9 presents the control chart of the residuals obtained for potency over a period of about 7 months. A single point was obtained beyond the lower control limit. No cause could be assigned to this event, and the residuals obtained for the subsequent sample fell within control limits. Other than this single point, no statistically significant trends (i.e. run rules violations) were observed. No adjustments were made to NIR potency calibration curve since it was initially established, 6 months prior to the start of this analysis for drift. During this time, the instrument source lamp was replaced twice. These data demonstrated remarkable stability of the NIR instrument over a period of more than 1 year.

Fig. 10 shows the control chart obtained in an analysis of the residuals for the lipid methods for these same samples. While no points were ob-

tained beyond the upper/lower control limits, statistically significant trends were observed. This was not surprising since the data were not truly independent. Multiple gravimetric method results were obtained with the same batch of extractant; preparation of the extractant was known to be a significant source of variation. A +2.0 mg/g average residual (NIR higher than gravimetric) was obtained during the first 3 months. No cause could be assigned to this bias, but the stability of the potency residuals suggested that instrument drift was not the cause. This suggested that either the sample matrix had changed since the lipid calibration was established or the gravimetric method had drifted. To compensate for this apparent bias, the NIR calibration curve was bias adjusted using the results from 30 of these samples tested consecutively just prior to adjustment. The slope of the calibration curve was not adjusted at this time. Following this adjustment, the average residual for the subsequent four months was +0.2 mg/g, which was not statistically significantly different from zero.

4. Conclusions

A rapid and precise method for measurement of potency and lipid content in monensin fermentation broth samples by near-infrared transmission spectroscopy was developed and validated. We believe this may be the first publication describing the use of NIR to quantify an ionophore. Since monensin does not absorb UV above 210 nm, to provide adequate sensitivity, the HPLC potency method utilizes a post-column reaction with vanillin, which adds complexity and contributes to method variability. Agitating the sample, filling a cuvette, and recording a NIR spectrum was a much more simple method providing essentially equivalent results. This same spectrum was utilized to simultaneously calculate a residual lipid concentration for which the standard method was time consuming and variable. Since the NIR analysis was complete in a few minutes, several replicate analyses could be completed in the time required for a single reference measurement. Thus, a signal-averaging strategy could be employed to provide a better measurement for improved control of the fermentor without requiring more laboratory resources.

The adequacy of the method, as well as which parameters were important to control, was established by rigorous method validation studies. Results of these studies showed the NIR method to be comparable in performance to the reference methods. Selectivity of the NIR method was established by examination of spectra obtained for the monensin reference standard and an oil reference sample, and identifying wavelengths where these analytes absorbed. Using these characteristic wavelengths, two multiple linear regression calibrations were developed allowing quantitation of potency and lipids from the same first-derivative NIR sample spectrum. Selectivity studies demonstrated excellent specificity for monensin in the presence of the oil, and a small, but acceptable effect of spiked monensin on NIR lipid method results. Validating the linearity of the method, a correlation coefficient of 0.992 was obtained for potency, and 0.903 for lipid content, over the concentration ranges of interest. The accuracy of the NIR method was validated by demonstrating that NIR results for 30 fermentation broth samples not utilized for calibration were not statistically significantly different than the laboratory reference method results. The standard deviation of the NIR method was estimated to be 1.20 mg/g for potency and 1.36 mg/g for lipid, which compared favorably with the precision of the reference methods.

As a strategy to detect drift in the measurement system during a period of 7 months, one sample per day was tested with both the NIR method and the reference methods. During this period, results of these comparison samples demonstrated that the NIR calibration for potency was stable. Established 6 months prior to this study, no calibration adjustments were needed for more than 1 year. This stability was remarkable, considering this length of time and that the instrument source lamp was changed twice during this time. Following collection of lipid data for the first 3 months, the NIR lipid calibration was adjusted for a 2 mg/g bias (NIR greater than laboratory reference). Results obtained following this adjustment

indicated no statistically significant bias between the two lipid methods.

5. Limitations and future plans

The influence of changes in monensin potency on the lipid result was one of the limitations of this work. Alternative calibration wavelengths and/or methods (e.g. partial least-squares) might be developed to overcome this limitation. Variability in the reference method for lipid content caused difficulty in developing the NIR calibration for lipids. An alternative approach, such as an unbiased regression method, could be utilized to better handle variability in both the NIR and reference lipid measurement.

While the precision study indicated that the NIR method was more precise than the laboratory reference methods for both potency and lipids, the study data was limited. Due to concerns about sample stability, the day-to-day component of the NIR measurement variation could not be estimated. To better understand the NIR method precision, a more rigorous study should be undertaken.

Acknowledgements

The authors wish to acknowledge B.M. McGarvey for many helpful discussions toward appreciating the limitations of linear regression analyses. L.K. Bristow, J. Burton, M.C. Davis, D. Deal, L.B. Griswold, C.L. Hartman, C.D. Hatten, M.L. Knox, A.N. Shouse, M.D. Southwick, D.A. Tully, and H.T. Tyler are acknowledged for their participation in collection of the data. M.W. Borer, R.W. Roller, and J.D. Hofer are acknowledged for providing scientific review of the manuscript prior to its publication.

References

[1] G. Vaccari, E. Dosi, A. Trilli, A. Gonzales-Vara, Semin. Food Anal. 3 (1998) 191–215.
[2] G. Macaloney, J.W. Hall, M.J. Rollings, I. Draper, K.B. Anderson, J. Preston, B.G. Thompson, B. McNeil, Bioprocess Eng. 17 (1997) 157–167.
[3] T. Yano, T. Aimi, Y. Nakano, M. Tamai, J. Ferment. Bioeng. 84 (5) (1997) 461–465.
[4] P.J. Brimmer, J.W. Hall, Can. J. Appl. Spectrosc. 38 (6) (1993) 155–162.
[5] S.V. Hammond, I.K. Brookes, Proc. Int. Biotechnol. Symp. Exp. 9th (1992) 325–333.
[6] R.A. Forbes, M.L. Persinger, D.R. Smith, J. Pharm. Biomed. Anal. 15 (3) (1996) 315–327.
[7] M.A. Arnold, J.J. Burmeister, G.W. Small, Anal. Chem. 70 (1998) 1773–1781.
[8] M.E. Haney, M.M. Hoehn. Antimicrob. Agents Chemother. (1967) 349–352.
[9] H.H. Willard, L.L. Merritt, Jr, J.A. Dean, Instrumental Methods of Analysis, 5th ed., Van Nostrand Company, New York, 1974, pp. 82–83 (Chapter 45).
[10] H. Martens, T. Naes, Multivariate Calibration, Wiley, New York, 1989 (Chapter 2).
[11] M. Blanco, J. Coello, H. Iturriaga, S. Maspoch, E. Rovira, J. Pharm. Biomed. Anal. 16 (1997) 255–262.
[12] Reference Manual for Near Infrared Spectral Analysis Software (NSAS), NIRSystems, Inc., Silver Spring, MD, 1993, Chapter 3, pp. 3-18–3-26.
[13] Reference Manual for Near Infrared Spectral Analysis Software (NSAS), NIRSystems, Inc., Silver Spring, MD, 1993, Appendix 1, pp. A-1-16–A-1-17.
[14] J.M. Rodewald, J.W. Moran, A.L. Donoho, M.R. Coleman, J. AOAC Int. 75 (1992) 272–279.
[15] R.H. Myers, Classical and Modern Regression with Applications, 2nd ed., Duxbury Press, Belmont, CA, 1990, pp. 357–358 (Chapter 7).
[16] J. Mandel, The Statistical Analysis of Experimental Data, Dover Publications, New York, 1984, pp. 288–292 (Chapter 12).
[17] D.J. Sheskin, The Handbook of Parametric and Nonparametric Statistical Procedures, CRC Press, New York, 1997, pp. 273–274 (Chapter 12).